Harada *et al. Earth, Planets and Space (2018) 70:152*
https://doi.org/10.1186/s40623-018-0923-4

Earth, Planets and Space

EXPRESS LETTER

Open Access

Temporal changes in inflation sources during the 2015 unrest and eruption of Hakone volcano, Japan

Masatake Harada*, Ryosuke Doke, Kazutaka Mannen, Kazuhiro Itadera and Mikio Satomura

Abstract

Global navigation satellite system data from Hakone volcano, central Japan, together with GEONET data from the Geospatial Information Authority of Japan, were used to investigate the processes associated with the volcanic activity in 2015, which culminated in a small phreatic eruption in late June 2015. Three deep and shallow sources, namely spherical, open crack, and sill, were employed to elucidate the volcanic processes using the observed GNSS displacements, and the MaGCAP-V software was used to estimate the volumetric changes of these sources. Our detailed analysis shows that a deep inflation source at 6.5 km below sea level started to inflate in late March 2015 at a rate of ~ 9.3×10^4 m^3/day until mid-June. The inflation rate then slowed to ~ 2.1×10^4 m^3/day and ceased at the end of August 2015. A shallow open crack at 0.8 km above sea level started to inflate in May 2015 at a rate of 1.7×10^3 m^3/day. There was no significant volumetric change in the shallow sill source during the volcanic unrest, which is evident from interferometric synthetic aperture radar analysis. The inflation of the deep source continued even after the eruption without a significant slowdown in inflation rate. The inflation stopped in August 2015, approximately 1 month after the eruption ceased. This observation implies that the transportation of magmatic fluid to a deep inflation source (6.5 km) triggered the 2015 unrest. The magmatic fluid may have then migrated from the deep source to the shallow open crack. The phreatic eruption was then caused by the formation of a crack that extended to the surface. However, steam emissions from the vent area during and after the eruption were apparently insufficient to mitigate the internal pressure of the shallow open crack.

Keywords: GNSS, Magma chamber, Hydrothermal system, Open crack, Phreatic eruption, Hakone

Introduction

Phreatic eruptions are the result of perturbations of the volcanic hydrothermal system (e.g., Barberi et al. 1992). Recent phreatic eruptions in the Japanese Islands have caused significant human casualties, with 61 fatalities during the September 27, 2014, Mt. Ontake eruption and one fatality during the January 23, 2018, Mt. Kusatsu Shirane eruption. Monitoring and forecasting are often difficult because the signals, such as excitation processes, are often subtle, which have severe implications for human safety (e.g., Kato et al. 2015).

Hakone volcano, located in the central part of Honshu Island, central Japan, recently generated a small phreatic eruption on June 29, 2015, at the Owakudani fumarole area, which is the largest fumarolic area on the volcano (Fig. 1). Although there were no fatalities, the volcanic activity caused serious human safety concerns since the area is an internationally famous sightseeing location in Japan, with many visitors to the fumarole area year-round. Furthermore, the elevated fumarolic activities caused serious damage to some of the steam wells that are used to make hot springs for the surrounding hotels, and these hotels were forced to temporarily stop providing hot springs to their visitors, resulting in significant economic losses to the area. Therefore, although the phreatic eruption was not a large event, its impact raised an important question regarding how intensively

---

*Correspondence: harada@onken.odawara.kanagawa.jp
Hot Springs Research Institute of Kanagawa Prefecture, 586 Iriuda, Odawara, Kanagawa 250-0031, Japan

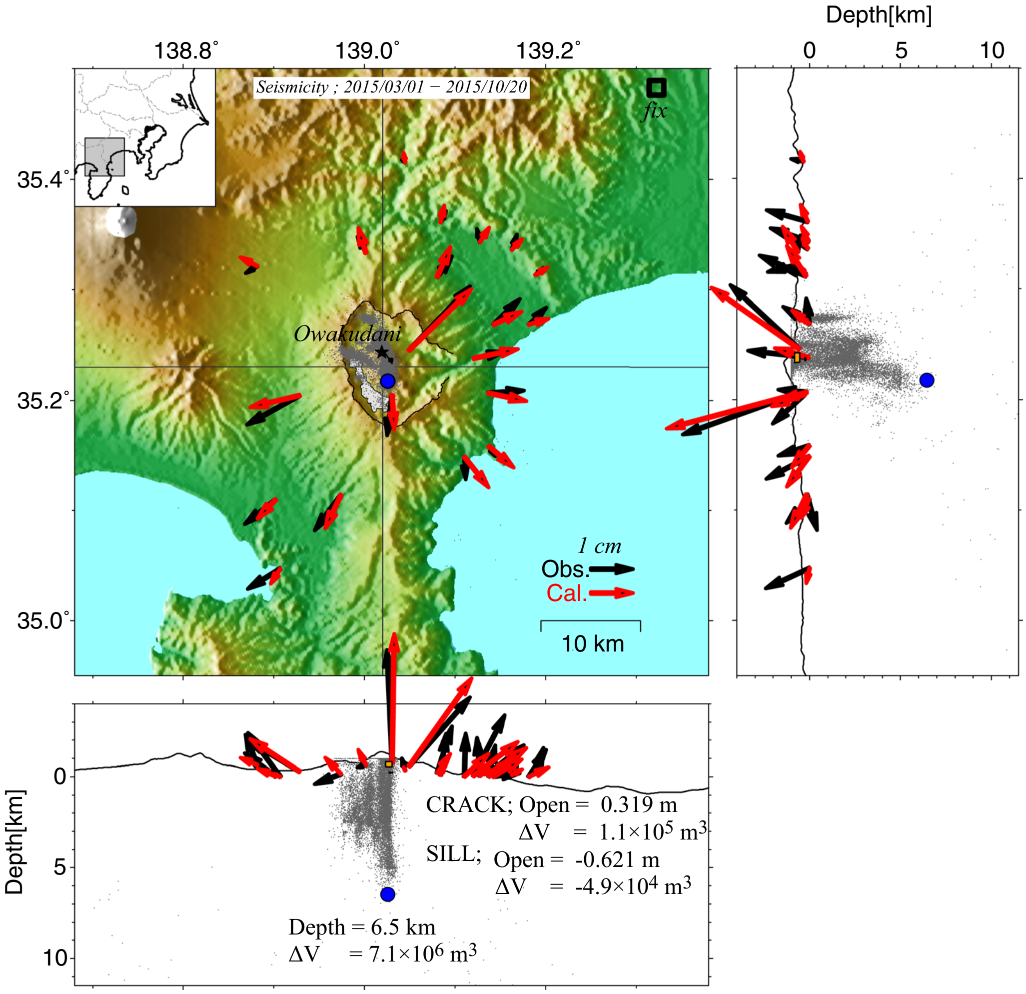

Fig. 1 Vectors indicating the GNSS movements associated with the 2015 unrest of Hakone volcano (black), and those calculated from the deep inflation source (red). Estimated deep inflation source is shown in blue circle. Two other shallow sources are shown in small squares. The gray dots represent seismicity from March 1 to October 20, 2015. The star shows the location of Owakudani

the volcano should be monitored to evaluate the risk of an eruption and mitigate the disasters related to the eruption.

The Hot Springs Research Institute of Kanagawa Prefecture (HSRI) has monitored Hakone volcano since 1989 using a seismometer array to detect seismic activities, GNSS and tiltmeters to detect crustal deformations, and gas sensors to observe fumarolic activities. Here, we use the GNSS data to examine the temporal changes in ground deformation and then attempt to elucidate how volcanic processes at depth, which we model as hydraulic processes, influenced the observed volcanic activity from April to September 2015.

Hakone volcano has a long eruption history, extending more than 400 kyr and including caldera-forming eruptions from 250 to 60 kyr ago (Takada et al. 2007). The most recent magmatic activity took place along a N–S trending line that traverses the center of the volcano, forming several small stratovolcanoes and lava domes. The seismic activity along the line appears to be related to a hydrothermal activity (Yukutake et al. 2011). The seismic activity of the volcano is relatively high, even during its inactive period, and several earthquakes, most of which are $M \leq 1$, are observed in a given month.

We have observed major earthquake swarm activities accompanied by the inflation of the volcano since the installation of the GNSS monitoring network in the 1990s (Harada et al. 2010). As shown in Fig. 2, such volcanic unrest has been observed in 2001, 2006, 2008–2009, 2013, and 2015. With the exception of the volcanic unrest in 2001 and 2015, these observed volcanic episodes were only accompanied by earthquake

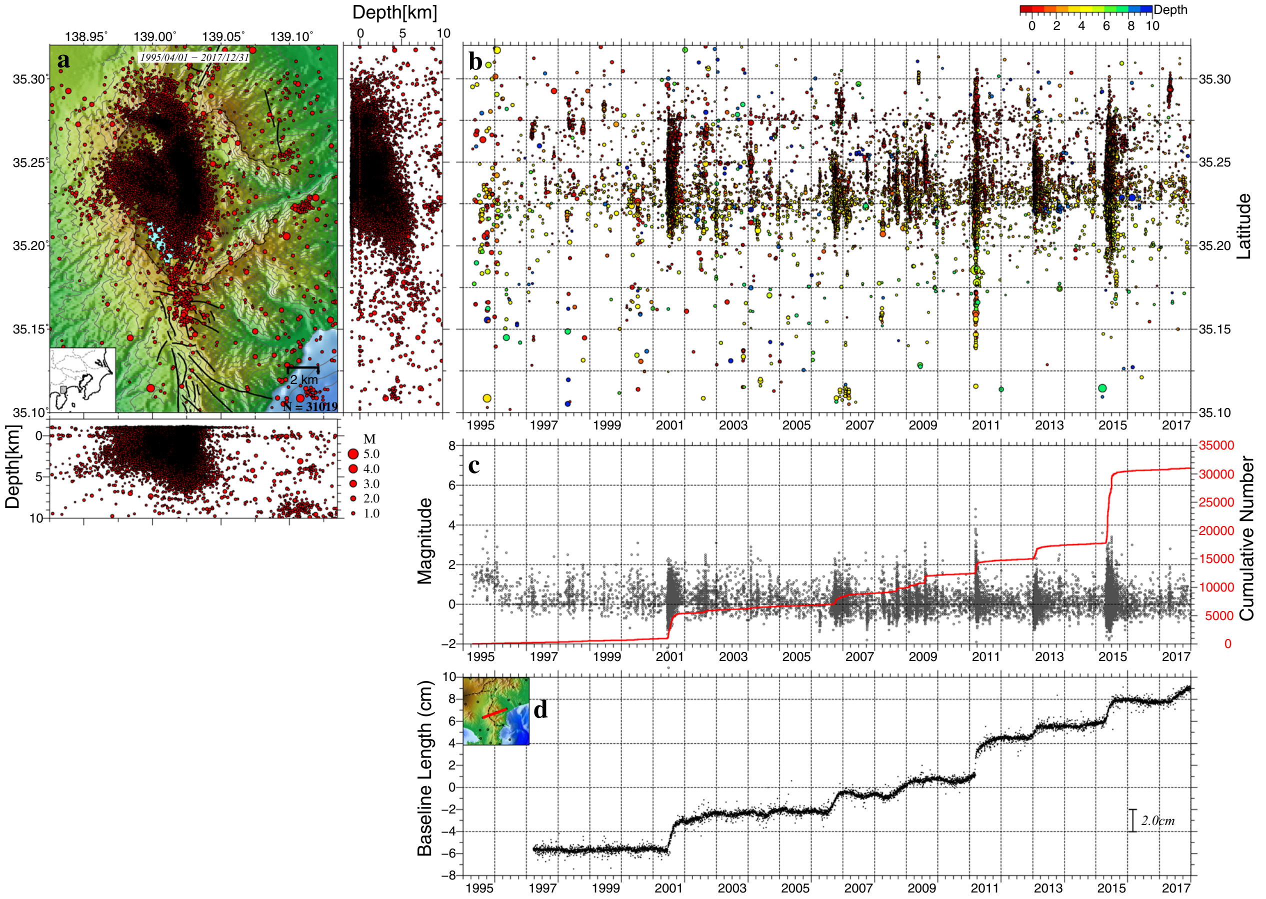

Fig. 2 Seismic activity and inflation of Hakone volcano from April 1995 to December 2017. The hypocenters were determined by HSRI. **a** Hypocentral distribution of Hakone volcano. **b** Spatiotemporal seismicity change. The vertical axis represents latitude. **c** Magnitude–time diagram and cumulative number of earthquakes. **d** Baseline length change between the Odawara and Susono-2 GEONET stations. The major volcanic earthquake swarm periods were observed in 2001, 2006, 2008–2009, 2013, and 2015. The elevated seismic activity in 2011 was triggered by the 2011 Tohoku Earthquake (M9.0)

swarms and inflation of the volcano. However, the 2001 unrest was accompanied by intensified steaming activity, and the 2015 event, which is discussed here, culminated in a small phreatic eruption.

The 2015 activity was first recognized by the GNSS network prior to mid-April as an inflation of the volcanic edifice. The earthquake swarm activity began in late April, and the steaming activity intensified in early May in Owakudani (Harada et al. 2015). Although the seismic activity declined since early June, there was a sudden and significant increase on the morning of June 29 that culminated in a small phreatic eruption (Yukutake et al. 2017; Mannen et al. 2018). Here, we estimate the locations of the inflation sources and their inflation rates during the 2015 volcanic activity based on GNSS data analysis.

GNSS data and location of inflation sources

Here, we used GNSS data from 20 observation stations in and around the volcano (Fig. 1). Ten stations are maintained by HSRI, with the other ten GEONET stations installed by the Geospatial Information Authority of Japan (GSI). One of the HSRI stations, located 2 km west of Owakudani, was excluded from the analysis because unrelated landslide movement appears to have contaminated the data from this station. Here, GNSS data from March 1, 2015 to June 30, 2016 were analyzed. The daily coordinates of the HSRI stations and one GEONET station were determined by our routine analysis using Bernese ver. 5.0 software (Dach et al. 2007) with IGS (International GNSS Service) precise ephemerides (Doke et al. 2018b). Furthermore, we used the F3 solution released by GSI to obtain the daily coordinates of the GEONET stations. We needed to combine the two network solutions since the coordinate estimations were conducted independently between HSRI and GSI. We therefore first calculated the offset of the three-dimensional (3D) coordinates at the commonly occupied observation station at Odawara (GEONET station code: 950230) and then subtracted the daily offsets from each of the HSRI sites, relying on the GSI F3 solution. We derived the coordinated time series at each of the sites from the obtained 3D coordinates, with velocity vectors estimated from the difference between the average coordinates for March 1–10, 2015 and the average coordinates for October 11–20, which are shown in Fig. 1.

We assumed three inflation sources in the shallow crust to estimate the potential sources that may have caused the observed crustal deformation associated with the volcanic activity (see Fig. 1). Our preliminary evaluation suggested a single inflation source at ~ 5.4 km depth that reasonably reconstructed the surface dislocation (root-mean-square (RMS) error $= 1.2 \times 10^{-3}$). However, an interferometric synthetic aperture radar (InSAR) analysis implied that a crack opened at shallow depths in the volcano during the phreatic eruption (Doke et al. 2018a). They also implied the existence of a deflation sill at ~ 250 m above sea level, which appears to deflate during the eruption and is assumed to be the source of the hydrothermal fluid that erupted. In this study, we employed the three sources obtained by the following procedure (Table 1; Fig. 3). In our model, we used locations of the open crack and deflation sill deduced by InSAR analysis (Doke et al. 2018a) and then estimated the location of the deep source based on the MaGCAP-V software (Fukui et al. 2013). We used the inverse analysis function of this software by first defining the initial values and deviations of the models for GNSS data at each observation site. We then obtained the optimal solution using a least squares method and weighting factors, where we assigned a weight of 1.0 to the two horizontal components and 0.2 to the vertical component.

The optimal solution, which yields the best fit location and inflation volume during the 2015 volcanic unrest, is shown in Table 1. We estimated a deep spherical inflation source beneath the central cone at ~ 6.5 km below sea level and a volume change of 7.1×10^6 m^3 (RMS error $= 2.0 \times 10^{-3}$). This deep source corresponds to the low seismic Vp/Vs region detected via tomographic analysis (Yukutake et al. 2015). Yukutake et al. (2015) suggested that this deep region contained a developed hydrothermal system.

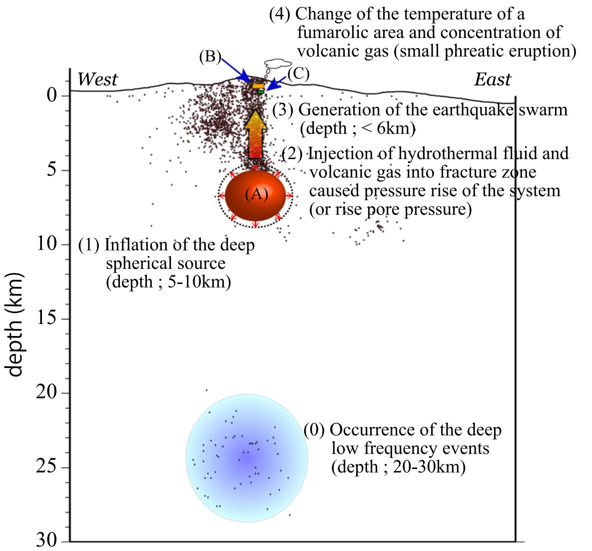

Fig. 3 Conceptual diagram of the 2015 unrest of Hakone volcano. (A), (B), and (C) are the inflation sources listed in Table 1. These sources are depicted as larger than the actual sizes for visualization

Calculation of the inflated volume during unrest

We estimated the temporal changes in the inferred volume of each source position during the 2015 volcanic unrest and eruption. The locations of the three sources listed in Table 1 were fixed such that only the volume changes of the three sources were calculated via the MaGCAP-V inversion analyses, with the same weights given to the horizontal and vertical components as in the previous analyses. The initial position of each GNSS station was fixed as the origin, which was determined as the average of the coordinates over the March 1–10 period, about one and a half months prior to the onset of the volcanic unrest. The 10-day average positions of the GNSS

Table 1 Parameters of the assumed sources

	Longitude (°)	Latitude (°)	depth (below sea level in m)	Length (m)	Width (m)	Strike (°)	Dip (°)	Opening (m)	Volume change (m^3)
(A) Spherical source	139.025872	35.217863	6466.5	–	–	–	–	–	7.1×10^6
(B) Crack	139.030707	35.233585	−827.6	1192.1	298.6	323.83	88.52	0.3186	1.1×10^5
(C) Sill	139.027414	35.235381	−224.9	261.4	304.1	0.00	0.00	−0.6210	-4.9×10^4

The crack and sill parameters are based on Doke et al. (2018a) stations were calculated for each 3-day shift (e.g., March 4–13 and March 7–16), with the initial position of the station origin subtracted from its 10-day averaged station positions to obtain the displacements from the origin. The resultant displacements at the GNSS stations were then used to estimate the volume changes of the three inflation sources. The best fit volume changes of the inflation sources are shown in Fig. 4. Note that the plots are at the last day of the selected 10-day intervals for monitoring purposes (which means that we cannot take the average using the "future" data).

Results

The inflation of the deep spherical source, labeled (A) in Fig. 3, appears to have started in late March 2015 (Fig. 4). The inflation rate does not appear to have been stable during the initial phase, with the volume change rates estimated via linear regressions of four intervals during this initial phase. First, there was a rapid increase of 7.9×10^4 m^3/day from late March to early April, which then slowed to 2.4×10^4 m^3/day in early to mid-April. The deep source underwent another rapid inflation at ~ 9.3×10^4 m^3/day from late April to mid-June. The deep source appeared to be relatively stable after mid-June, with another inflation after the eruption, which occurred from June 29 to July 1. This inflation continued until the end of August at ~ 2.1×10^4 m^3/day.

The inflation of the shallow open crack source, labeled (B) in Fig. 3, appears to have started gradually in mid-May and continued until early August at an inflation rate of 1.7×10^3 m^3/day. It is noteworthy that there was no rate change for this source that was related to the eruption. This shallow open crack source appears to have deflated slowly after mid-September at 0.4×10^3 m^3/day.

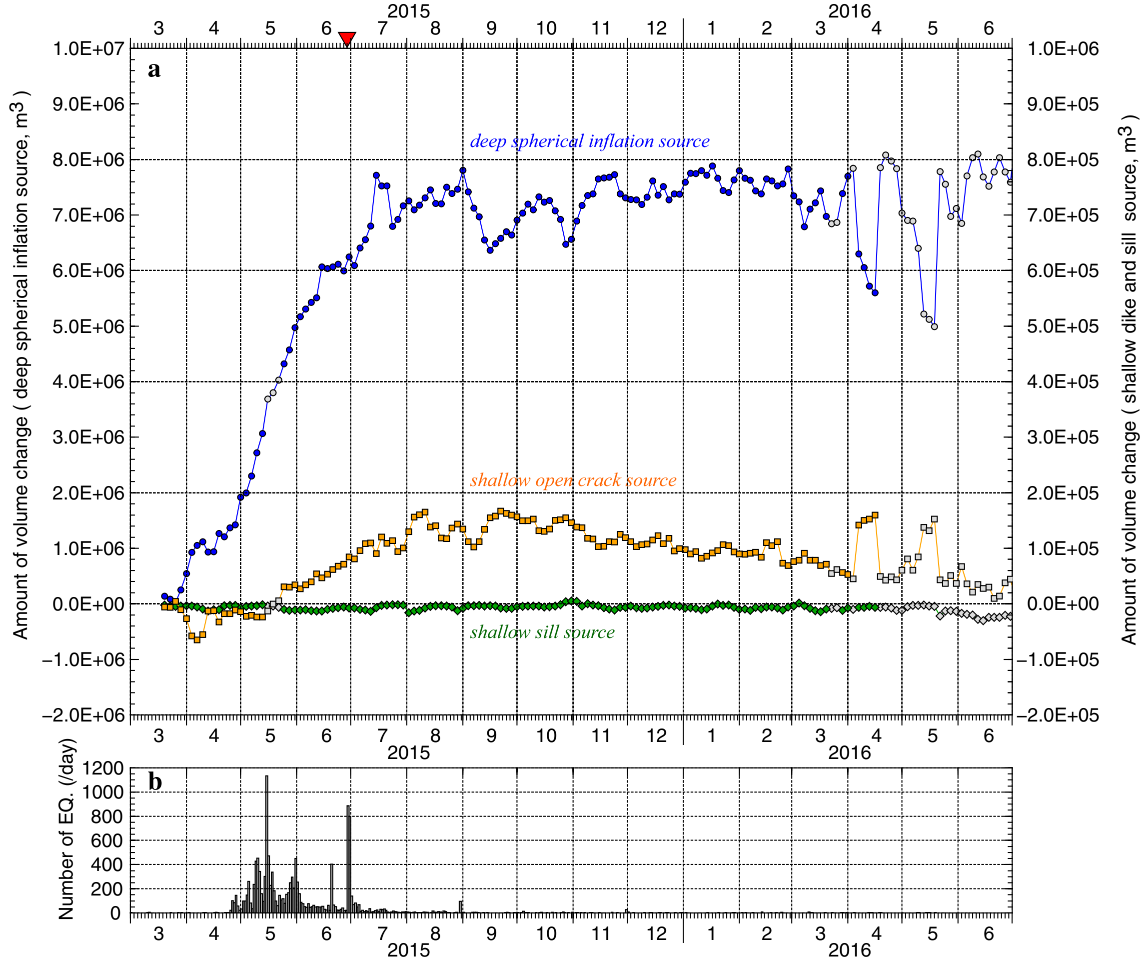

Fig. 4 **a** Volume changes of the three sources before and after the 2015 volcanic unrest at Hakone volcano (from March 2015 to June 2016). The blue, orange, and green symbols are the total volume changes of the deep spherical inflation, shallow open crack, and sill sources, respectively. Gray plots mean that an estimated error is large (RMS error ≥ 3.0×10^{-3}). **b** Daily number of earthquakes at Hakone volcano during the same period as above

Although fluctuations are still evident in the last stage, after April 2016, these may be due to the unstable solution of the inversion since the RMS error for this period (3.0×10^{-3}) is much larger than the other periods. The deflation pattern continued until June 2016, but the volcanic crustal deformation subsequently became obscured by the tectonic movements of the Philippine Sea Plate.

The inflation of the shallow sill source, labeled (C) in Fig. 3, showed no significant contribution to the crustal deformation detected by this GNSS analysis. We consider that the sparse GNSS observation network was unable to detect such a local and small sill in the shallow crust in the Hakone volcano region.

Discussion

Our GNSS analysis detected the inflation of a deep spherical source in late March 2015, well before the onset of the seismic swarm activity in late April. It is interesting to note that a deep low-frequency event (DLF) began at approximately the same time as the inflation (Yukutake and Abe 2018; Mannen et al. 2018). However, the DLF occurred at 15–30 km depth, much deeper than the deep spherical source at 5–6 km depth (see Fig. 3). Yukutake and Abe (2018) hypothesized that the DLF event may be due to an increase in magmatic fluid pressure. This suggests that such fluid may have migrated to shallower depths, potentially generating inflation of the deep spherical source discussed here.

The inflation of the deep source initially ceased by mid-April but was later reactivated. The second inflation in late April appears to coincide with the April 26 onset of the earthquake swarm. This sequence is potentially related to the inflation of a hydrothermal system beneath the volcano due to the injection of hydrothermal fluids separated from the underlying magma chamber. It is expected that this injection increased the pore fluid pressure within the fracture zone and enhanced the shallow seismic activity (Yukutake et al. 2011), coinciding with the shallow inflation that initiated in late May. The continued shallow inflation during the post-eruption period notably persists after the eruption, indicating that the eruption did not ease the pore pressure to stop inflation beneath the volcano.

Here, an open crack, which is indicated by a set of InSAR images before and after the eruption (June 18–July 2 and June 7–July 5 pairs; Doke et al. 2018a), represents the shallow inflation source. As shown above, the shallow inflation began in mid-May. However, the inflation of the open crack prior to June 18 was unclear in the InSAR images. We therefore consider the shallow inflation as an inflation of the fracture system beneath the volcano instead of an open crack inflation.

The inflations in the deep spherical and shallow open crack sources appear to have ceased in late August. Late August may be considered the end of the hydrothermal fluid injection from the deep magma source since there was significantly reduced seismic activity prior to August. The shallow open crack then began to deflate from mid-September. We interpret the crack deflation as the withdrawal of hydrothermal fluid due to closure of the crack or fracture system. The hydrothermal fluid may have been released to the surface gradually from the newly formed fumarole area in Owakudani just above the open crack.

However, there is no evidence of deep source deflation, which is evident from the unchanged baseline length (Fig. 2d). The lack of deflation at depth indicates that the deep spherical source remained inflated. Magma intrusion within the crust (~ 6.5 km below sea level) could also be possible, but there are no other observations to support this hypothesis. We surmise that the lack of deflation implies the accumulation of magma and/or hydrothermal fluid at depth. Since accumulation of hydrothermal fluid and magma could be a preparatory process of larger eruptions in the future (e.g., Murase et al. 2016), volume change monitoring and hydrothermal system modeling in this depth range are critically important in the eruption forecasting of Hakone volcano.

Conclusion

We considered potential inflation sources beneath Hakone volcano at crustal depth and monitored their volume changes over the course of the precursory, eruptive, and post-eruptive phases of the 2015 eruption. The rapid inflation from late March implies the transportation of magmatic fluid into a mid-crustal magma chamber, as inferred from the contemporaneous deep low-frequency seismic events. After a short intermission in April, the deep source resumed to inflate, accompanied by a seismic activity, and continued until August. The inflation that also initiated from mid-May in the shallow source region may be due to the injection of hydrothermal fluid into the hydrothermal system above the magma chamber. This injection continued until August, and the late June phreatic eruption was not enough to mitigate the pore pressure of the hydrothermal system. The fluid injection appeared to cease in August, and the shallow source then began to deflate. However, no significant change was observed in the deep source volume. Therefore, an accumulation of magma and/or fluid may have continued to persist in the deep source area. This accumulation may be a preparatory process for a future eruption, such that intense monitoring and modeling of the magma-hydrothermal system are critically important for forecasting and disaster mitigation measures to better prepare for future eruptions.

Abbreviations

DLF: deep low-frequency event; GEONET: GNSS Earth Observation Network System; GNSS: Global Navigation Satellite System; GSI: Geospatial Information Authority of Japan; HSRI: Hot Springs Research Institute of Kanagawa Prefecture; IGS: International GNSS service InSAR, interferometric synthetic aperture radar; RMS: root-mean-square.

Authors' contributions

MH engaged in the GNSS analysis and drafted the manuscript. RD processed the GNSS data and determined the daily coordinates of our original GNSS sites. KM, KI, and MS assisted in the study and edited the manuscript. All authors read and approved the final manuscript.

Acknowledgements

The authors would like to acknowledge the helpful support of Dr. Akio Yoshida, Dr. Ryou Honda, Dr. Yohei Yukutake, Dr. Yuki Abe, and Dr. Teruyuki Kato. Gratitude is extended to the Geospatial Information Authority of Japan for providing the GNSS data used in this study. We used the MaGCAP-V software (Fukui et al. 2013) for the analysis. This manuscript was greatly improved by constructive comments from two anonymous reviewers and Editor Mitsuhiro Nakagawa.

Competing interests

The authors declare that they have no competing interests

Availability of data and materials

The data that support the findings of this study are available upon request from the corresponding author, with the exception of the GEONET data, which are available through the GSI Web site.

Consent for publication

Not applicable.

Ethics approval and consent to participate

Not applicable.

Funding

This study was implemented as an ordinary research project of HSRI.

Publisher's Note

Received: 28 March 2018 Accepted: 14 September 2018

References

Barberi F, Bertagnini A, Landi P, Principe C (1992) A review on phreatic eruptions and their precursors. J Volcanol Geotherm Res 52:231–246. https://doi.org/10.1016/0377-0273(92)90046-G

Dach R, Hugentobler U, Fridez P, Meindl M (2007) Bernese GPS Software Version 5.0. Astronomical Inst. Univ., Bern, p 612

Doke R, Harada M, Mannen K, Itadera K, Takenaka J (2018a) InSAR analysis for detecting the route of hydrothermal fluid to the surface during the 2015 phreatic eruption of Hakone Volcano, Japan. Earth Planets Space 70:63. https://doi.org/10.1186/s40623-018-0834-4

Doke R, Harada M, Miyaoka K (2018b) GNSS observation and monitoring of the Hakone Volcano and the 2015 unrest. J Disaster Res 13:526–534. https://doi.org/10.20965/jdr.2018.p0526

Fukui K, Ando S, Fujiwara K, Kitagawa S, Kokubo K, Onizwa S, Sakai T, Shimbori T, Takagi A, Yamamoto T, Yamasato H, Yamazaki A (2013) MaGCAP-V: Windows-based software to analyze ground deformation and geomagnetic change in volcanic areas. IAVCEI 2013 Scientific Assembly, Kagoshima, pp 2C–P8

Harada M, Hosono K, Ito H, Aketagawa T, Kobayashi A, Honda R, Yukutake Y, Yoshida A (2010) Swarm activity and crustal deformation in Hakone. Programme and abstracts of the Volcanological Society of Japan 2010 Fall Meeting, p 29 (**in Japanese**)

Harada M, Itadera K, Honda R, Yukutake Y, Doke R (2015) Earthquake swarm activities and crustal movement of the 2015 volcanic event at Hakone Volcano (Rapid results). Bull Hot Springs Res Inst Kanagawa Pref 47:1–10 **(in Japanese with English abstract)**

Kato A, Terakawa T, Yamanaka Y, Maeda Y, Horikawa S, Matsuhiro K, Okuda T (2015) Preparatory and precursory processes leading up to the 2014 phreatic eruption of Mount Ontake, Japan. Earth Planets Space 67:111. https://doi.org/10.1186/s40623-015-0288-x

Mannen K, Yukutake Y, Kikugawa G, Harada M, Itadera K, Takenaka J (2018) Chronology of the 2015 eruption of Hakone volcano, Japan—geological background, mechanism of volcanic unrest and disaster mitigation measures during the crisis. Earth Planets Space 70:68. https://doi.org/10.1186/s40623-018-0844-2

Murase M, Kimata F, Yamanaka Y, Horikawa S, Matsuhiro K, Matsushima T, Mori H, Ohkura T, Yoshikawa S, Miyajima R, Inoue H, Mishima T, Sonoda T, Uchida K, Yamamoto K, Nakamichi H (2016) Preparatory process preceding the 2014 eruption of Mount Ontake volcano, Japan: insights from precise leveling measurements. Earth Planets Space 68:9. https://doi.org/10.1186/s40623-016-0386-4

Takada A, Mannen K, Ukawa M, Chiba T (2007) Fuji and Hakone Volcanoes, field trip guidebook cities on Volcanoes 5 conference. Bull Volcanological Soc., Japan, p 41p

Yukutake, Y, Abe Y (2018) Deep low-frequency earthquakes beneath Hakone volcano, central Japan, and their relation to the volcanic activity, JpGU Meeting 2018, SVC41-03

Yukutake Y, Ito H, Honda R, Harada M, Tanada T, Yoshida A (2011) Fluid-induced swarm earthquake sequence revealed by precisely determined hypocenters and focal mechanisms in the 2009 activity at Hakone volcano, Japan. J Geophys Res 116:B04308. https://doi.org/10.1029/2010JB008036

Yukutake Y, Honda R, Harada M, Arai R, Matsubara M (2015) A magma-hydrothermal system beneath Hakone volcano, central Japan, revealed by highly resolved velocity structures. J Geophys Res Solid Earth 120(5):3293–3308

Yukutake Y, Honda R, Harada M, Doke R, Saito T, Ueno T, Sakai S, Morita Y (2017) Analyzing the continuous volcanic tremors detected during the 2015 phreatic eruption of the Hakone volcano. Earth Planets Space 69:164. https://doi.org/10.1186/s40623-017-0751-y